Phonons, Rotons, and Layer Modes of Liquid ^{4}He in Aerogel

B. Fåk* and O. Plantevin
Département de Recherche Fondamentale sur la Matière Condensée, SPSMS/MDN, CEA Grenoble, 38054 Grenoble, France

H. R. Glyde and N. Mulders
Department of Physics and Astronomy, University of Delaware, Newark, Delaware 19716
(Received 15 March 2000)

We report the first observation of two-dimensional layer modes in both fully filled and partially filled aerogel. Using complementary high-energy resolution and high statistical precision neutron scattering instruments, and two different 87% porous aerogel samples, we show that the three-dimensional (3D) phonon-roton excitation energies and lifetimes of liquid ^{4}He in aerogel are the same as in bulk ^{4}He within current precision. The layer modes are the excitations that distinguish aerogel from the bulk rather than a difference in the 3D roton energy.

PACS numbers: 67.40.–w, 61.12.Ex

Liquid ^{4}He confined in porous media such as aerogel and Vycor are model examples of bosons in disorder and in confined geometries [1,2]. Disorder and confinement has a profound impact on superfluidity, Bose-Einstein condensation, and phase transitions [1–3]. The nature of the excitations in these "dirty Bose systems" in turn plays a key role in determining these properties, and measurements of these excitations by neutron scattering has now begun [4–10].

In this Letter, we present a new picture of the excitations of liquid ^{4}He in aerogel. Our new neutron scattering measurements using two different neutron spectrometers and two different 87% porous aerogel samples show that there is no difference between the three-dimensional (3D) phonon-roton (p-r) excitation energies and lifetimes of superfluid ^{4}He in aerogel and in bulk liquid ^{4}He within current precision. Specifically, the temperature (T) dependence of the 3D roton energy, and of other excitation energies, in aerogel is indistinguishable from that in the bulk. Previous measurements have reported that the T dependence of the roton energy in aerogel does differ from that in the bulk and that this difference accounts for the different temperature dependence of the superfluid density in aerogel [5]. We observe for the first time two-dimensional (2D) layer modes propagating in the liquid layers adjacent to the aerogel walls not observed in any previous measurements in aerogel [4–8]. The new picture is that the 3D p-r energies of superfluid ^{4}He in aerogel are the same as in bulk ^{4}He, but aerogel supports 2D layer modes for wave vectors in the roton region which have rotonlike dispersion lying approximately 1 K below the 3D roton energy: At full filling of the aerogel, the intensity in the layer mode is 20% of the 3D p-r intensity in the roton region. The new feature of superfluid ^{4}He in aerogel that distinguishes it from the bulk is the layer modes rather than the temperature dependence of the roton energy.

To reveal the dynamical features that distinguish ^{4}He in aerogel from bulk ^{4}He, we made complementary neutron scattering measurements with high-energy resolution and with high statistical precision on denser (87% porous) aerogel to increase the effects of disorder and confinement. Precision measurements of the temperature dependence of the 3D roton energy were made using high-resolution spectrometers and simultaneous measurement in the bulk. We observe layer modes near the roton wave vector as additional intensity at energies below the 3D p-r excitations on both spectrometers. The unambiguous identification of the additional intensity as layer modes is obtained here, for the first time in any porous material, by measuring the dynamic structure factor $S(Q, \omega)$ as a function of filling.

Aerogel is a highly tenuous structure of irregularly connected silica (SiO_2) strands with a large distribution of pore sizes, from a few to a few hundred Å, and a mean free path of typically 1000 Å [11]. The present 87% porous aerogel samples were prepared in a standard base-catalyzed process followed by hypercritical drying. The samples were grown directly in the stainless steel cells of 13.6 mm inner diameter used for the neutron scattering experiments. This eliminates voids between the aerogel and the walls of the cell where bulk liquid could otherwise collect. To reduce the elastic incoherent scattering from hydrogen impurities, present as OH^- groups attached to the strands, the aerogels were deuterated. Different methods were used for the two samples studied. One sample (A) was first baked in vacuum at high temperatures and then flushed with D_2 gas at high pressures. This treatment was repeated several times. The other sample (B) was made from fully deuterated chemicals. The latter method reduces the elastic scattering by a factor of 2–3 compared to the former. The samples were handled in an inert atmosphere and not exposed to air. A ^{3}He refrigerator was used for the measurements, where the thermometers had previously been calibrated against the ^{3}He vapor pressure.

Most of the measurements near the roton wave vector were performed on the IN12 triple-axis spectrometer at the ILL high-flux reactor, using sample B. A higher

 0031-9007/00/85(18)/3886(4)$15.00

energy resolution (46 μeV at the roton) than in our previous measurements [6] was achieved by using an incident neutron energy of 3.1 meV and 40′ collimations, in combination with a pyrolytic graphite (002) monochromator and analyzer. A Be filter in the incident beam removed the second-order harmonics from the monochromator. Complementary measurements were performed using the "A" sample on the IN6 time-of-flight spectrometer (ILL) with an incident energy of 3.1 meV and an energy resolution of 110 μeV, covering wave vectors between 0.4 and 2.1 Å^{-1}. The measurements on both spectrometers were performed for temperatures between 0.5 and 2.3 K, the latter being above the bulk superfluid transition temperature $T_\lambda = 2.17$ K.

Figure 1 shows $S(Q, \omega)$ of fully filled aerogel at wave vectors in the roton region. $S(Q, \omega)$ consists of a large *p-r* excitation peak plus additional intensity at energies below the *p-r* peak. The additional intensity is broad, approximately 2–3 times the energy resolution, and it could correspond to one broad or several sharp excitations. In order to determine the origin of the additional intensity, we have measured the filling dependence of $S(Q, \omega)$ at the roton wave vector on IN12. Figure 2 shows $S(Q, \omega)$ for five different fillings. The integrated intensity in the main 3D roton peak and in the additional contribution is shown in Fig. 3. Intensity in both components of $S(Q, \omega)$ is observed first at approximately 30% filling, corresponding to three helium layers on the aerogel surface. The first two layers are believed to be solid. The integrated intensity of the 3D roton increases linearly with filling up to 100% filling as expected for a 3D bulk mode. The intensity of the additional component increases initially with filling but saturates at higher fillings, as expected for a layer mode. This shows that the additional intensity originates from the first few liquid layers close to the aerogel surface. Its intensity as a function of the number n of filled layers is well described by the empirical expression introduced by Thomlinson *et al.* [12],

$$I(n) = I_\infty\{1 - \exp[-(n - n_0)/\zeta]\}. \quad (1)$$

A best fit of Eq. (1) to our data, shown as a line in Fig. 3, is obtained for $n_0 = 2.7$ and $\zeta = 3.6$ layers. Thus, the intensity of the layer mode begins at approximately 2.7 layers (0.7 liquid layers) and propagates within the following 3.6 layers. The layer mode saturates to an intensity I_∞ that is 20% of the 3D roton intensity.

As noted, the aerogel sample used on IN12 was grown with deuterated chemicals, which reduces the multiple scattering (inelastic scattering in liquid ^{4}He plus additional elastic scattering from the aerogel that changes the wave vector) to 2% of the roton peak height. At the roton wave vector, the multiple scattering will be centered above the roton energy, since the roton is the lowest-energy excitation. The phonon intensity is too weak to give any substantial multiple scattering contribution, as shown by our Monte Carlo simulations. Hence, the additional intensity

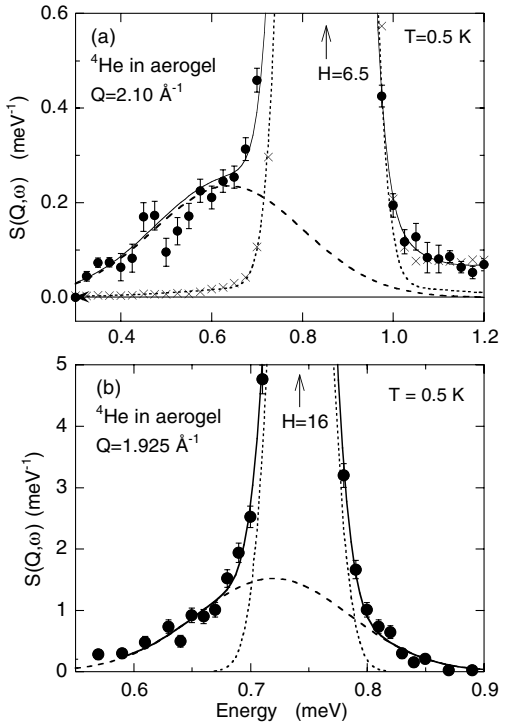

FIG. 1. Dynamic structure factor of superfluid ^{4}He at $T = 0.5$ K in 87% porous aerogel (closed circles with error bars) near the roton wave vector. The solid line is a fit to the aerogel data of the sum of a sharp bulk excitation (dotted line) and an additional contribution at lower energies (dashed line) arising from layer modes. The scattering at energies above the main peak is due to multiparticle (multiphonon) excitations. The value of the peak height is given by H. (a) Sample A measured on IN6 with an energy resolution of 110 μeV at a wave vector $Q = 2.1$ Å^{-1}. Data for bulk ^{4}He is shown by crosses. (b) Sample B measured on IN12 with an energy resolution of 46 μeV at $Q = 1.95$ Å^{-1}.

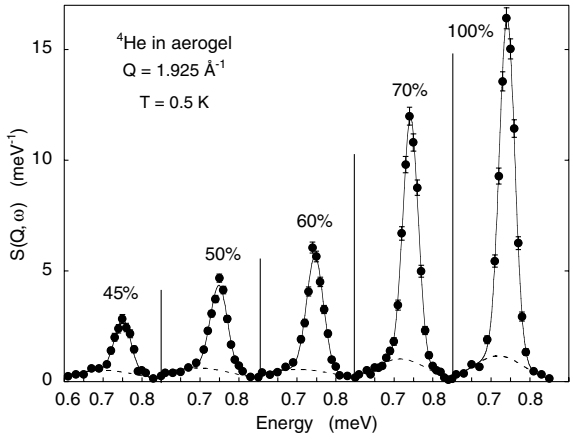

FIG. 2. Dynamic structure factor of superfluid ^{4}He at $T = 0.5$ K in 87% porous aerogel (sample B) at the roton wave vector $Q = 1.925$ Å^{-1} for five different fillings between 45% and 100%, measured on IN12 with an energy resolution of 46 μeV. The solid line is a fit to the data of a sum of a sharp (resolution-limited) bulklike excitation and an additional contribution at lower energies (dashed line) due to layer modes.

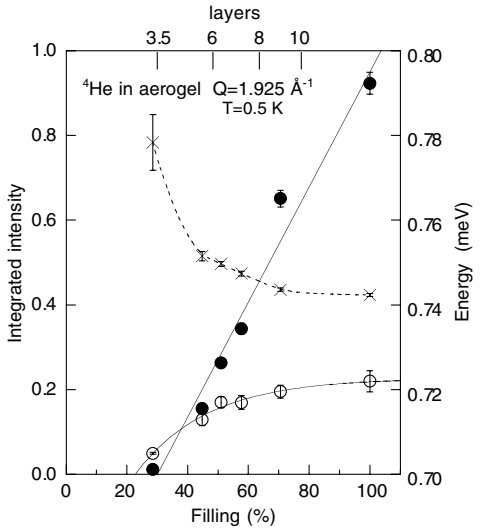

FIG. 3. Integrated intensity of the 3D bulklike roton (closed circles) and the 2D layer mode (open circles) in superfluid ^{4}He in 87% porous aerogel at $T = 0.5$ K as a function of filling. The solid lines show a linear fit to the 3D mode and a fit of Eq. (1) to the 2D mode. The crosses show the energy of the 3D bulklike roton. The dashed line is a guide to the eye.

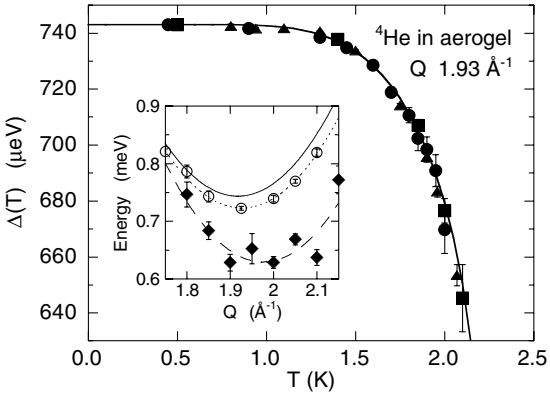

FIG. 4. Temperature dependence of the bulklike roton energy in different aerogel samples (symbols) compared to bulk ^{4}He (line). Circles: aerogel with 87% porosity measured on IN12 with an energy resolution of 46 μeV; triangles: aerogel with 87% porosity measured on IN6 with an energy resolution of 110 μeV; squares: aerogel with 95% porosity measured on IN12 with an energy resolution of 110 μeV (from Ref. [6]). The inset shows the energy dispersion near the roton wave vector of the bulklike mode (solid line) and of the layer modes measured on IN12 (open symbols) and on IN6 (solid symbols). The curves show the best fits to a parabolic dispersion.

attributed to 2D layer modes near the roton cannot arise from multiple scattering.

The energy of the 3D bulklike mode decreases slightly with increasing filling toward the bulk value, as can be seen from the crosses in Fig. 3. Since the roton energy in *bulk* helium decreases with increasing pressure, the higher energy at low fillings observed here could suggest that the density is lower in the partially filled sample.

The inset of Fig. 4 shows the energy of the peak position of the 3D bulk and of the 2D layer modes as a function of wave vector in the roton region measured in sample A on IN6 and in sample B on IN12. The 3D *p-r* energy in fully filled aerogel is the same as in bulk liquid ^{4}He. The energies of the 2D layer modes measured in sample B on IN12 and in sample A on IN6 are not the same and two 2D mode energies are shown in Fig. 4. Because of the weak intensity of these modes, it is difficult to determine whether the layer modes are indeed somewhat different in the two aerogel samples used, or whether it is an instrumental effect. It is clear that the mode observed on IN12 lies too close to the main bulklike peak to be resolved in the measurements on IN6, where the resolution was 2 times coarser. On the other hand, the statistical precision on IN6 is better than that on IN12 and the mode intensity can be observed to lower energies on IN6.

The energy dispersion curves of the layer modes are well described by the parabolic form $\omega_Q = \Delta + (Q - Q_R)^2/2\mu$, used for the bulklike *p-r* modes, as shown by lines in the inset of Fig. 4. The gaps Δ of the two layer modes in the present aerogel samples, 0.63(1) and 0.72(1) meV, are similar but larger than that in Vycor, 0.55(1) meV [10], or for films on graphon, 0.54–0.6 meV [12–14]. The "roton mass" μ is the same for all excitations within statistical precision, while the position of the roton Q_R is increased from 1.925 to 1.98 for the lower (0.63 meV) layer mode. The intensity in the layer modes increases significantly between the roton $Q = 1.925$ Å^{-1} and $Q = 2.1$ Å^{-1}. No additional intensity was observed on IN6 for wave vectors below 1.7 Å^{-1}, and on IN12 we did not measure below this Q value.

Figure 4 shows the temperature dependence of the energy of the bulklike roton in different fully filled aerogel samples observed on different spectrometers: the present 87% porous aerogel samples on IN12 (IN6) with an energy resolution of 46 (110) μeV and a previous 95% porous aerogel on IN12 with an energy resolution of 110 μeV [6]. Measurements of bulk ^{4}He were also made in the same setup, using the same cryostat with calibrated thermometers. The temperature dependence of the roton energy in these aerogels is in excellent agreement with that of the bulk roton, shown as a line in Fig. 4 represented using the parametrization by Bedell *et al.* [15]. Hence, within precision, there is no difference between the roton energy in helium in aerogel and bulk helium at any temperature. Although this result is in disagreement with some earlier work [5], we believe that our finding is correct, as it has been observed for different aerogels measured on different spectrometers using well calibrated thermometers and simultaneous measurements on bulk ^{4}He.

Anderson *et al.* [7] showed that the intrinsic line width of the roton in aerogel at low temperatures ($T \leq 1.2$ K) is the same as in bulk liquid ^{4}He. We find that the temperature dependence of the roton linewidth in all aerogel

samples investigated is also the same as in bulk ^{4}He within the instrumental resolution. The slight broadening reported in our initial measurements [6] vanishes if the additional intensity of the layer modes observed in the tail of the bulklike roton (see Fig. 1) is subtracted.

Layer modes propagating in both free liquid ^{4}He films and adjacent to aerogel, Vycor and graphite walls have been predicted [14,16–19] and inferred from superfluid density and specific heat measurements [2,19,20]. They have been observed directly on graphon/graphite surfaces [12–14] and in Vycor [9,10]. The layer mode roton energy in aerogel observed here (0.63–0.72 meV) is significantly higher than that in Vycor and on graphon. Since the 2D roton energy is predicted to increase with decreasing film density [16,18], this suggests that the density of liquid layers in aerogel is less than in Vycor or on graphon. We observe no layer mode below $Q = 1.7$ Å^{-1}. This is consistent with the predictions of Clements *et al.* [14,17] and Krotscheck [18] that the intensity in 2D modes decreases as Q decreases below the roton Q.

We have not observed any deviations of the Q dependence of the *p-r* energy, and in particular no indication of a gap as $Q \rightarrow 0$. Gaps can arise from localization of the liquid ^{4}He by disorder [21]. We also did not observe any dispersionless modes as have been observed in liquid ^{4}He on graphon. Dispersionless modes are predicted for flat substrates only [18]. We have not seen any reduction in the phonon energy due to disorder as has been predicted for strong disorder [22,23]. As noted, we have found new additional low-energy modes, the layer modes. Such modes at lower energy have indeed been predicted by simulations of liquid ^{4}He in three dimensions [24] and simulations of 2D hard-core bosons on a lattice [23] in the presence of disorder.

In conclusion, the 3D phonon-roton excitations of superfluid ^{4}He in aerogel for porosities between 87% and 95% are the same as in bulk liquid ^{4}He. There are additional 2D excitations in the ^{4}He layers near the aerogel walls. These layer excitations distinguish superfluid ^{4}He in aerogel from the bulk.

We thank the cryogenics laboratory at the Institut Laue-Langevin for the loan of the ^{3}He refrigerator, M. DePalma for technical assistance, and H. Schober for assistance with the complementary measurements on IN6. IN12 is operated by KFA Juelich and CEA Grenoble. This work was partially supported by the National Science Foundation, Grant No. DMR 96-23961.

*Present address: ISIS Facility, Rutherford Appleton Laboratory, Chilton, Didcot, Oxon OX11 0QX, England.

[1] M. H. W. Chan *et al.,* Phys. Rev. Lett. **61**, 1950 (1988); G. K. S. Wong *et al.,* Phys. Rev. Lett. **65**, 2410 (1990).
[2] J. D. Reppy, J. Low Temp. Phys. **87**, 205 (1992).
[3] G. M. Zassenhaus and J. D. Reppy, Phys. Rev. Lett. **83**, 4800 (1999).
[4] J. de Kinder, G. Coddens, and R. Millet, Z. Phys. B **95**, 511 (1994); G. Coddens, J. de Kinder, and R. Millet, J. Non-Cryst. Solids **188**, 41 (1995).
[5] P. E. Sokol *et al.,* Nature (London) **379**, 616 (1996); R. M. Dimeo *et al.,* Phys. Rev. Lett. **79**, 5274 (1997); M. R. Gibbs *et al.,* J. Low Temp. Phys. **107**, 33 (1997).
[6] O. Plantevin *et al.,* Phys. Rev. B **57**, 10 775 (1998).
[7] C. R. Anderson *et al.,* Phys. Rev. B **59**, 13 588 (1999).
[8] R. T. Azuah, H. R. Glyde, J. R. Beamish, and M. A. Adams, J. Low Temp. Phys. **117**, 113 (1999).
[9] R. M. Dimeo *et al.,* Phys. Rev. Lett. **81**, 5860 (1998).
[10] H. R. Glyde *et al.,* Phys. Rev. Lett. **84**, 2646 (2000).
[11] J. V. Porto and J. M. Parpia, Phys. Rev. B **59**, 14 583 (1999).
[12] W. Thomlinson, J. A. Tarvin, and L. Passell, Phys. Rev. Lett. **44**, 266 (1980).
[13] H. J. Lauter *et al.,* Phys. Rev. Lett. **68**, 2484 (1992); J. Low Temp. Phys. **87**, 425 (1992).
[14] B. E. Clements *et al.,* Phys. Rev. B **53**, 12 242 (1996).
[15] K. S. Bedell, D. Pines, and A. Zawadowski, Phys. Rev. B **29**, 102 (1984).
[16] J. Halinen, V. Apaja, K. A. Gernoth, and M. Saarela, J. Low Temp. Phys. (to be published).
[17] B. E. Clements *et al.,* Phys. Rev. B **50**, 6958 (1994), and references therein.
[18] E. Krotscheck (private communication).
[19] M. Chester and L. Eytel, Phys. Rev. B **13**, 1069 (1976).
[20] D. F. Brewer, in *The Physics of Liquid and Solid Helium,* edited by K. H. Benneman and J. B. Ketterson (Wiley, New York, 1978), Pt. II, p. 573.
[21] W. Krauth and N. Trivedi, Europhys. Lett. **14**, 627 (1991); W. Krauth, N. Trivedi, and D. M. Ceperley, Phys. Rev. Lett. **67**, 2307 (1991).
[22] L. Zhang, Phys. Rev. B **47**, 14 364 (1993).
[23] M. Makivic, N. Trivedi, and S. Ullah, Phys. Rev. Lett. **71**, 2307 (1993).
[24] M. Boninsegni and H. R. Glyde, J. Low Temp. Phys. **112**, 251 (1998).